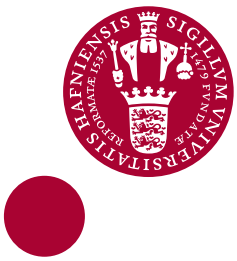

Estimation of herbaceous fuel moisture content using vegetation indices and land surface temperature from MODIS data

Sow, Momadou; Mbow, Cheikh; Hely, Christelle; Fensholt, Rasmus; Sambou, Bienvenu

Published in:
Remote Sensing

DOI:
10.3390/rs5062617

Publication date:
2013

Document version
Publisher's PDF, also known as Version of record

Remote Sens. **2013**, *5*, 2617-2638; doi:10.3390/rs5062617

OPEN ACCESS

Remote Sensing

ISSN 2072-4292

www.mdpi.com/journal/remotesensing

Article

Estimation of Herbaceous Fuel Moisture Content Using Vegetation Indices and Land Surface Temperature from MODIS Data

Momadou Sow [1,2,3,*], Cheikh Mbow [1,†], Christelle Hély [2,‡], Rasmus Fensholt [4] and Bienvenu Sambou [1]

[1] Institut des Sciences de l'Environnement (ISE), Faculté des Sciences et Techniques, Université Cheikh Anta Diop de Dakar, B.P. 5005 Dakar-Fann, Sénégal; E-Mails: c.mbow@cgiar.org (C.M.); bienvenu.sambou@ucad.edu.sn (B.S.)

[2] Centre Européen de Recherche et d'Enseignement des Géosciences de l'Environnement (CEREGE), Université Aix-Marseille III, CNRS UMR 7330, Europôle de l'Arbois, B.P. 80, F-13545 Aix-en-Provence cedex 4, France; E-Mail: christelle.hely-alleaume@univ-montp2.fr

[3] Laboratoire d'Enseignement et de Recherche en Géomatique (LERG), Ecole Supérieure Polytechnique (ESP)/FST, Université Cheikh Anta Diop de Dakar, B.P. 5005 Dakar-Fann, Sénégal

[4] Section of Geography, Department of Geosciences and Natural Resource Management, Faculty of Science, University of Copenhagen, Oster Voldgade 10, 1350 Copenhagen K, Denmark; E-Mail: rf@geo.ku.dk

† Current Address: ICRAF (World Agroforestry Centre), SD6 United Nations Avenue, P.O. Box 30-677 Gigiri, Kenya

‡ Current Address: Centre de Bio-Archéologie et Ecologie (CBAE), Laboratoire Paléoenvironnements et Chronécologie (PALECO), Ecole Pratique des Hautes Etudes, UMR 5059, Institut de Botanique, 163 rue A. Broussonnet, F-34090 Montpellier, France

* Author to whom correspondence should be addressed; E-Mail: momadou@yahoo.fr; Tel.: +221-77-152-56-60.

Received: 21 March 2013; in revised form: 25 April 2013 / Accepted: 25 April 2013 / Published: 24 May 2013

Abstract: The monitoring of herbaceous fuel moisture content is a crucial activity in order to assess savanna fire risks. Faced with the difficulty of managing wide areas of vegetated surfaces, remote sensing appears an attractive alternative for terrestrial measurements because of its advantages related to temporal resolution and spatial coverage. Earth observation (EO)-based vegetation indices (VIs) and the ratio between Normalized Difference Vegetation Index (NDVI) and surface temperature (ST) were used for

assessment of herbaceous fuel moisture content estimates and validated against herbaceous data collected in 2010 at three open savanna sites located in Senegal, West Africa. EO-based estimates of water content were more consistent with the use of VI as compared to the ratio NDVI/ST. Different VIs based on near-infrared (NIR) and shortwave infrared (SWIR) reflectance were tested and a consistent relationship was found between field measurements of leaf equivalent water thickness (EWT) from all test sites and Normalized Difference Infrared Index (NDII), Global Vegetation Moisture Index (GVMI) and Moisture Stress Index (MSI). Also, strong relationships were found between fuel moisture content (FMC) and VIs for the sites separately; however, they were weaker for the pooled data. The correlations between EWT/FMC and VIs were found to decrease progressively as the woody cover increased. Although these results suggest that NIR and SWIR reflectance can be used for the estimation of herbaceous water content, additional validation from an increased number of study sites is necessary to study the robustness of such indices for a larger variety of savanna vegetation types.

Keywords: herbaceous moisture content; vegetation indices; land surface temperature; remote sensing; MODIS; Senegal

1. Introduction

Savanna fires play a major role in ecosystem dynamics in dry tropical areas [1,2]. Due to an increased number of fires ignited by humans, fire frequency on savanna ecosystems has increased during the last decades to a level where it has become a threat to biodiversity and ecosystem stability [3]. Although the cause of ignition in most cases is related to rural livelihoods, the severity of a fire depends on many biophysical factors, such as vegetation water status, topography, and wind direction [4]. The vegetation fuel moisture is a critical parameter in fire ignition because flammability is closely limited by leaf water content [5]. Therefore, the monitoring of vegetation water content is fundamental in assessing the risk of fire [6–11]. Ground measurements of herbaceous water content are labor intensive and expensive if performed over larger areas and therefore difficult to apply at the regional scale. The phenology adds another level of complexity which is related to the short time window during which fuel moisture drop down rapidly (a few weeks after the end of the rainy season). To overcome these limitations, satellite remote sensing is suggested as an attractive solution due to large area coverage, high temporal frequency and non-destructive alternatives to expensive field measurements of vegetation water content [12–15].

Considering the varying spatial and temporal dynamics of vegetation biophysical variables such as canopy water content, the use of earth observation (EO) data is a great opportunity for acquiring real-time continuous information on vegetation status [13,14,16]. The estimation of vegetation water content from satellite data has been attempted using high and low spatial resolution sensors. The high resolution reduces noise in quantitative correlation with field data by providing a higher spatial accuracy [11,17]. However, the main constraint of using high or moderate spatial resolution data for vegetation monitoring is the low temporal resolution (e.g., revisit cycle of 16 days for Landsat) while

vegetation water content can vary with a significantly higher temporal frequency [18]. The low spatial resolution data offers a higher temporal resolution (e.g., daily or 10-daily) provided by high-temporal satellite sensors (e.g., Advanced Very High Resolution Radiometer—AVHRR; Moderate Resolution Imaging Spectroradiometer—MODIS; and *Satellite Pour l'Observation de la Terre*—SPOT VEGETATION) and are more likely to be used operationally since fire managers require frequent updates of water content [5,11]. The use of satellite remote sensing data for analysis of vegetation is traditionally based on the use of various spectral indices. The best known of these is the Normalized Difference Vegetation Index (NDVI) indicating the chlorophyll content of vegetation from the combined use of the red and near infrared wavebands [19]. NDVI has also been used as a proxy of vegetation water content in several studies based upon the assumption of chlorophyll content dependency of canopy water content [8,19–24]. This assumption may be correct for some conditions but cannot be generalized to all ecosystems [11,25]. Variations in chlorophyll content can be caused by water stress but also by normal phenological status of the plant, atmospheric pollution, nutrient deficiency, toxicity, plant disease, and radiation stress [26].

Since the mid-1990s, several studies [16,25,27–35] have focused on combining information from different wavelengths and showed the ability of near infrared (NIR) (0.7–0.9 μm) and short wave infrared (SWIR) (1.2–2.5 μm) to determine vegetation water content [25,28,30,31,36]. In addition to VIs, several studies have proven the potential use of combining NDVI and surface temperature (ST) for predicting vegetation moisture [5,37,38]. The primary basis for this relationship should be found in the unique spectral reflectance-emittance properties of plant leaves in the red and infrared wavelengths combined with the low thermal mass of plant leaves relative to soil. Plant spectral reflectance patterns provide a possibility to remotely sense surface variations in green biomass [39]. Similarly, transpiration and the limited thermal mass of plant leaves provides a possibility to distinguish between vegetation and soil background properties from thermal infrared observations [40]. Plant leaves actively exchange absorbed solar radiation through transpiration. During daylight hours, plant leaves (in the absence of water stress) maintain a temperature close to air temperature, whereas exposed, dry soil temperatures are much higher than air temperatures [41].

Studies on the monitoring of vegetation water content by remote sensing for fire risk assessment are numerous, and many have focused on ecosystems located in midlatitudes [29,42] and in North America [13,14,30]. Generally, these studies compared the ability of spectral approaches operating in the shortwave optical domain to predict vegetation water content across different plant functional types. These studies provided mostly encouraging results on the ability of remote sensing to monitor vegetation water content. Also, studies in Sahel covering a variety of open savanna ecosystems have been conducted [11,16,18,25,28,35]. The Sahel is characterized as a region highly affected by fire and where the monitoring of vegetation water content could potentially play an important role in the assessment of fire risk for subsequent fire management.

This study aims at testing relationships between vegetation indices based on (1) NIR/SWIR reflectance data, (2) the combined use of NDVI/ST and field measurements of herbaceous water content in the Senegalese savanna ecosystems, to assess the ability of remotely sensed information to predict herbaceous water content for improved fire risk assessment. Both daily and eight-day composite products from 2010 are tested to study the importance of image acquisition timeliness when monitoring a highly fluctuating biophysical variable like vegetation water content. Extensive

validation data, collected in the field, cover three different savanna types to account for spatial and ecological differences in the sensitivity of the indices tested. The focus in this study is on herbaceous vegetation water content, since most fires in the semi-arid to sub-humid areas are mainly surface fires fueled by the herbaceous vegetation layer.

2. Materials and Methods

2.1. Study Area

Three sites were selected following a north–south gradient taking into account the main eco-climatic regions of Senegal along an increasing rainfall gradient (Sahelian area, northern Sudanian area and southern Sudanian area (Figure 1).

Figure 1. MODIS (MCD12Q1) land cover classification and location of biomass sampling sites in the main ecosystems of Senegal (Source NASA: http://e4ftl01.cr.usgs.gov/MOTA/).

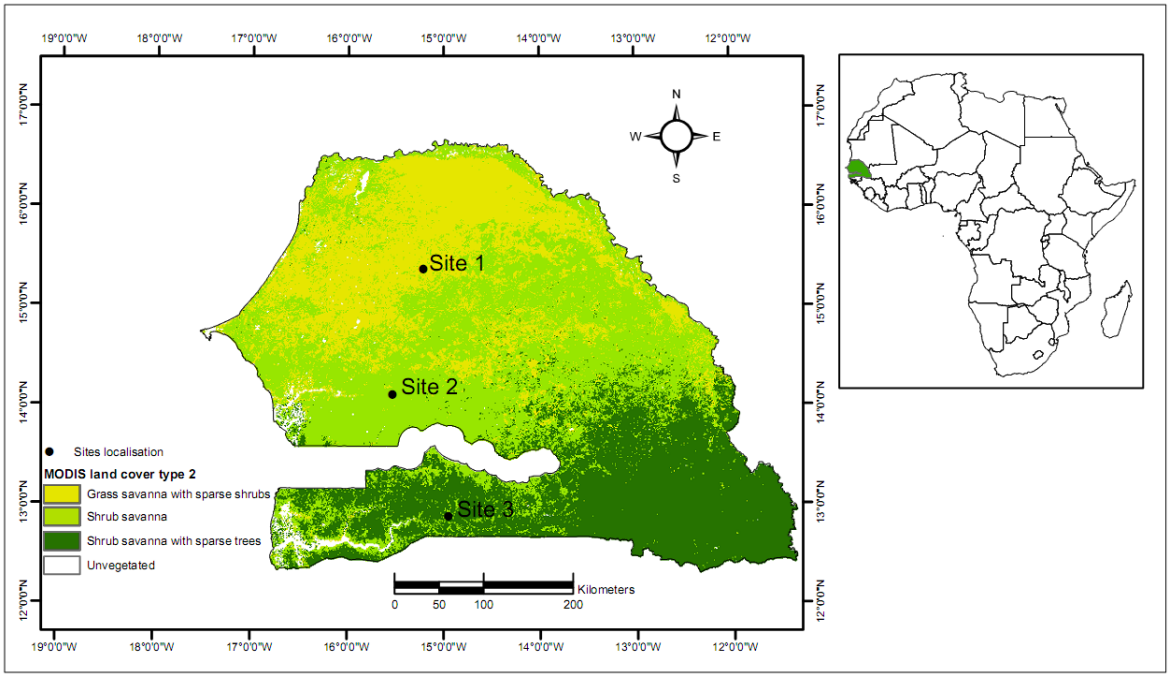

The first site is located at 15°16'3"N, 14°51'55"W near the village of Barkedji in the northern part of the country. In the central Sahel, the rainy season extended from July to September with annual rainfall ranging from 200 to 400 mm [16]. The length of the rainy seasons ranges changes from three to six months from northernmost to the southernmost site. Relative humidity can reach a minimum of 10% in the northern part (in May), as a consequence of high temperatures and high evaporating power of the region's hot and dry harmattan wind. In the early stages of the dry season, the harmattan winds primarily influence the northeast of Senegal before moving to the southern continental regions [43]. Conversely, the relative humidity can exceed 75% throughout the entire region when the summer monsoon starts in July. The annual mean of the maximum temperatures for the region is above 35 °C. The vegetation is a grassland (Figure 2) dominated by annual grasses: *Eragrostis gangetica*, *Eragrostis tremula*, *Schoenefeldia gracilis*, *Zornia glochidiata*, *Dactyloctenium aegyptium*,

Aristida mutabilis, *Cenchrus biflorus*, *Chloris virgata*, *Aristida fuiniculata* and *Polycarpea linearifolia*. The sparse woody layer is dominated by *Balanites aegyptiaca*, *Boscia senegalensis*, *Adenium obesum*. The woody cover did not exceed 11% [44], as determined by the method outlined by Mahamane and Saadou [45] based on physiognomy and floristic composition.

Figure 2. Composition and distribution of vegetation typical for the three sites: (**a**) grassland; (**b**) shrub savanna; (**c**) shrub savanna with sparse trees.

(**a**)

(**b**)

(**c**)

The second site is located at 13°52'59"N, 15°25'0"W near the village of Maka in central Senegal. Over the northern Sudanian region, the rainy season extended from June to October with annual rainfall ranging from 700 to 800 mm. The relative humidity ranges from 34% to 79%. The average annual temperature is *ca*. 29 °C. The savanna vegetation (Figure 2) includes shrub and tree species (*Combretum glutinosum*, *Guiera senegalensis*, *Sterculia setigera*, *Pterocarpus erinaceus* and *Cordyla pinnata*) with a total woody cover estimated to be 29% [44]. The herbaceous layer is continuous and dominated by *Andropogon pseudapricus*. However, we noted the presence of *Pennisetum pedicellatum*, *Spermacoce chaetocephala* and *Spermacoce stachydea*.

The third site is located at 12°49'0"N, 14°52'0"W near the village of Dioulacolon in the southern Sudanian area. During the rainy season (May to October), annual rainfall varies from 800 to

1,200 mm. The relative humidity ranges from 37%–89% and the annual mean temperature is *ca*. 28 °C. The landscape composition includes shrub savannas and woodlands with a continuous grass layer (Figure 2) dominated by *Andropogon pseudapricus*, *Ctenium villosum*, *Andropogon gayanus*, and *Indigofera leptoclada.* Woody vegetation is dominated by *Combretum glutinosum*, *Combretum nigricans*, *Strychnos spinosa*, *Crossopteryx febrifuga*, *Terminalia macroptera* and *Bombax costatum.* The total woody cover at this site is estimated to be close to 50% [44].

2.2. Experimental Design for Biomass Sampling

In each of the three sites, a quadratic experimental plot of 1 km^2 was established including nine sub-plots of 250 × 250 m (Figure 3).

Figure 3. The experimental design for biomass collection covered 1 km^2, including nine plots of 250 × 250 m from which four samples were collected at random locations using a 1 m^2 quadrat. The geographic coordinates of the MODIS 1 km^2 LST pixel corners were used to outline the experimental plot area for the best possible match of footprints from MODIS data and ground observations.

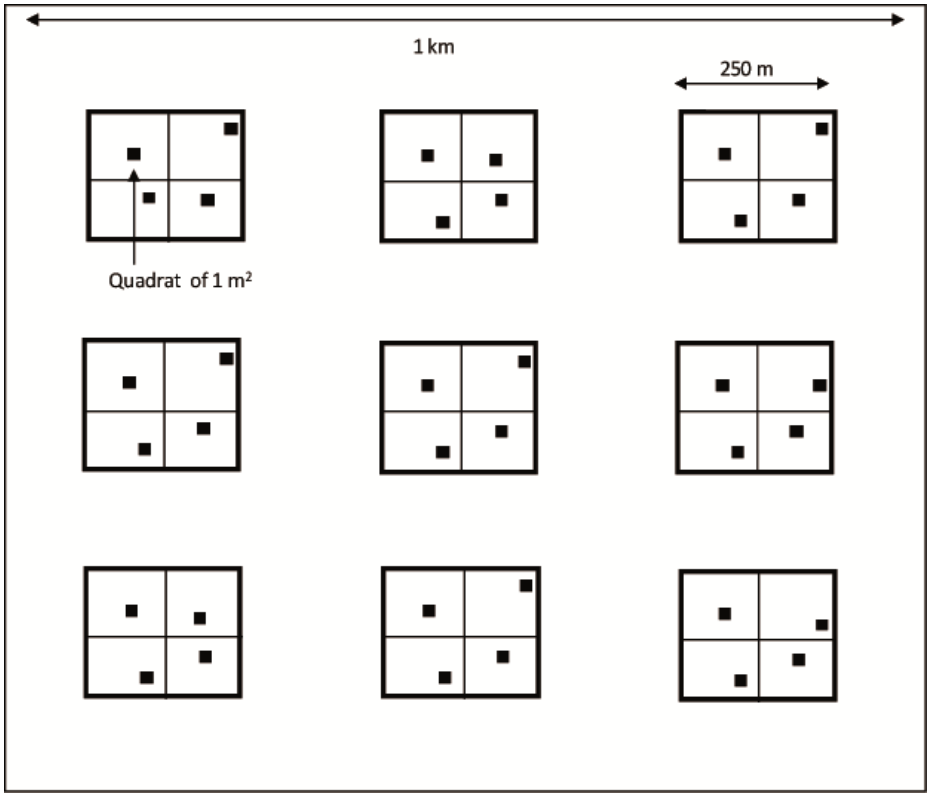

The specific location of the experimental plots was selected based on landscape physiognomy at the 1-km^2 level and the sub-plots were selected to include the dominant herbaceous species in the area. Measurements of herbaceous water content must occur at the right time and for the most representative grass cover, in order to properly capture the variations of water content that vary over space and rapidly declines at the end of the rainy season. Data collections were conducted in each site on a daily basis starting eight days after the last rain in 2010. This timing allowed comparing trends of water content for the three sites at the early dry-season. To be able to start the collection of biomass eight

days after the last rain, we used predictions (through a personal communication) of the potential period of the end of rainfall season in different areas of Senegal from the National Agency of Meteorology in Senegal (ANAMS). Due to the distance separating sites, three teams carried out the field work, simultaneously applying an identical methodological protocol. For 32 days, we conducted daily data collection at 14–15 h coinciding with the driest period of the day (Sow, unpublished data). Aboveground herbaceous biomass in each 1 m^2 quadrat was harvested. In each plot of 250 m, four samples were collected, and weighed directly in the field to avoid water loss [29]. The average of the four samples constituted the sample weight of fresh biomass in the plot and was disposed in a hessian bag before being oven-dried at 60 °C until constant dry weight was obtained [46,47].

The direct method for the estimation of the herbaceous water content was made on the basis of two different metrics: (i) the fuel moisture content [4,5,8,29,48] and (ii) the equivalent water thickness at leaf level [25,27–31,49–51]. *FMC* (Equation (1) [5,11,52]) is defined as the percentage of moisture content as compared to dry material weight as follows:

$$FMC = ((FW - DW) / DW) \times 100 \quad (1)$$

where *FW* is the fresh weight measured in the field and *DW* the oven dry weight of the same sample.

Similarly, leaf *EWT* is defined as the quantity of water per herbaceous unit area as follows (Equation (2) [29,47,52]):

$$EWT = (FW - DW) / A \quad (2)$$

where *A* is an estimation of the area covered by herbaceous and expressed in m^2 in the plot of 1 m^2 quadrat. *FMC* indicates the intrinsic moisture of the plants, while *EWT* indicates water content per unit surface area of the vegetation [29].

The average water content at the plot level was then compared to the VI of the corresponding geographic pixels. For the part of the analyses including comparisons to the eight-day MODIS data, daily field-based water content estimates were averaged to produce eight-day values.

2.3. MODIS Data and Processing

The Moderate Resolution Imaging Spectroradiometer (MODIS) surface reflectance product was used due to the high spectral and temporal resolution required for this study. The MODIS sensors onboard the Terra and Aqua platforms have daytime crossing over Senegal at about 10 h and 14 h, respectively. We selected the MODIS Aqua data for this study to minimize the time difference between satellite acquisition and the samples collected in the field (between 14 and 15 h). MODIS Collection 5 data were downloaded from the National Aeronautic and Space Administration (NASA) (http://reverb.echo.nasa.gov/reverb/). The different MODIS products used included both daily observations of surface reflectance and land surface temperature (98 scenes) and eight-day composites surface reflectance and land surface temperature (12 scenes) covering the period from 6 October to 23 November 2010 (Table 1).

Table 1. Characteristics of the MODIS products used in this study.

Product Short Name	Product Description	Year
MYD09GA	MODIS/Aqua Surface Reflectance Daily Level 2 Global 500 m SIN Grid Collection 5	2010
MYD11A1	MODIS/Aqua Land Surface Temperature/Emissivity Daily Level 3 Global 1 km SIN Grid Collection 5	2010
MYD09A1	MODIS/Aqua Surface Reflectance Eight-day Level 3 Global 500 m SIN Grid Collection 5	2010
MYD11A2	MODIS/Aqua Land Surface Temperature/Emissivity Eight-day Level 3 Global 1 km SIN Grid Collection 5	2010
MCD12Q1	MODIS/Terra + Aqua Land Cover Type Yearly Level 3 Global 500 m SIN Grid Collection 5	2010

Surface reflectance and land cover data products are available in a 500-m spatial resolution, whereas the land surface temperature (LST) product has a spatial resolution of 1 km. The MODIS data sets are provided in Sinusoidal (SIN) mapping grid. The MODIS data were therefore reprojected to Universal Transverse Mercator System (UTM) and re-sampled using Nearest Neighbor using the MODIS Reprojection Tool (MRT, see https://lpdaac.usgs.gov/tools/modis_reprojection_tool for download). The computing of spectral indices and statistical analyses were conducted using both the ENVI 4.5 and R software [53].

The daily MODIS and eight-day MODIS composite data products include a data quality assessment (QA-data) product providing information on overall usefulness and cloud condition on a per-pixel basis. For the daily MODIS reflectance observations (MYD09GA) the Reflectance Data State QA "cloud state" parameter was used (bit 0–1) to screen for clouds. "Clear" was considered cloud free, whereas "cloudy" and "mixed" were considered cloud contaminated. For the daily LST observations the Daytime LSTE quality control "Data quality flag" parameter was used to screen for clouds (bit 2–3). "Good quality" was considered cloud free, whereas "Other quality" was considered cloud contaminated. Only observations being labeled as cloud-free were used in this study.

Similarly, for the eight-day MODIS composite (MYD09A1), the 500-m Reflectance Band Quality "MODLAND QA bits" parameter was used (bit 0–1). "Corrected product produced at ideal quality all bands" was considered cloud free, whereas "corrected product produced at less than ideal quality for some or all bands" were considered cloud contaminated. For the eight-day LST composite, the quality control for daytime LST and emissivity "data quality flag" parameter was used to screen for clouds (bit 2–3). "Good data quality of L1B in 7 TIR bands" was considered cloud free, whereas "other quality data" was considered cloud contaminated.

2.4. Vegetation Indices

In this study, we focused on the vegetation indices combining the satellite channels in the NIR and SWIR. Ideally, a VI should be sensitive to the type of dynamics of the vegetation cover to be studied, insensitive to changes in the soil layer and affected by atmospheric effects to a minimum [25,54–58]. Variations in leaf internal structure and leaf dry matter content influence the SWIR reflectance, thereby rendering SWIR reflectance unsuitable for vegetation water content estimates if not combined

with information from other wavelengths. The combined use of NIR and SWIR makes it possible to normalize for the influence on the reflectance signal related to variations in leaf internal structure and leaf dry matter content. Several studies support the theory that ratios, or normalized ratios, of these wavebands suppress the effect of variation in leaf scattering [25,27,28,52]. The NIR reflectance is affected by leaf internal structure and leaf dry matter content but not by water content [16]. By combining the NIR with the SWIR reflectance information, variations induced by leaf internal structure and leaf dry matter content can be removed and thus improve the accuracy in retrieving the vegetation water content [25].

Several VIs have been proposed over the years as based on observations from different satellite sensor systems including measurements in the SWIR wavelengths (primarily Landsat, SPOT and MODIS). These indices focus on the characteristics of water absorption in the SWIR (sensitive to changes in leaf water content) and the NIR (sensitive to changes in leaf internal structure) of the spectrum being designed as ratios or normalized ratios of broad wavebands in the NIR and the SWIR. Amongst the most referred indices are Normalized Difference Water Index—NDWI [31,59], Normalized Difference Infrared Index—NDII [17,60–62], Simple Ratio Water Index—SRWI [59,63], Moisture Stress Index—MSI [61], and Global Vegetation Moisture Index—GVMI [28]. GVMI uses a combination of the SWIR and NIR channel rectified for contamination by atmospheric effects using the blue-band channel [28]. However, we did not rectify our NIR observations [13,52,64] because MODIS data used here have been atmospherically corrected [65,66]. The ability of these indices to estimate herbaceous water content was tested in this study from MODIS surface reflectance data using equations reported in Table 2.

Table 2. Algorithms for the computing of vegetation indices extracted from literature. MODIS Band 2 (center μm) = 0.858 μm; Band 5 = 1.240 μm; Band 6 = 1.640 μm; Band 7 = 2.130 μm. NDWI (Normalized Difference Water Index); NDII (Normalized Difference Infrared Index); SRWI (Simple Ratio Water Index); MSI (Moisture Stress Index); GVMI (Global Vegetation Moisture Index).

Index	Algorithm	References
$NDWI_{(2,5)}$	$NDWI = \frac{\rho_{NIR} - \rho_{SWIR}}{\rho_{NIR} + \rho_{SWIR}} = \frac{Band2 - Band5}{Band2 + Band5}$	[31,59]
$NDII_{(2,6)}$	$NDII = \frac{\rho_{NIR} - \rho_{SWIR}}{\rho_{NIR} + \rho_{SWIR}} = \frac{Band2 - Band6}{Band2 + Band6}$	[60–62]
$NDII_{(2,7)}$	$NDII = \frac{\rho_{NIR} - \rho_{SWIR}}{\rho_{NIR} + \rho_{SWIR}} = \frac{Band2 - Band7}{Band2 + Band7}$	[17,61]
$SRWI_{(2,5)}$	$SRWI = \frac{\rho_{NIR}}{\rho_{SWIR}} = \frac{Band2}{Band5}$	[59,63]
$MSI_{(6,2)}$	$MSI = \frac{\rho_{SWIR}}{\rho_{NIR}} = \frac{Band6}{Band2}$	[61]
$MSI_{(7,2)}$	$MSI = \frac{\rho_{SWIR}}{\rho_{NIR}} = \frac{Band7}{Band2}$	[61]
$GVMI_{(2,6)}$	$GVMI = \frac{(\rho_{NIR} + 0.1) - (\rho_{SWIR} + 0.02)}{(\rho_{NIR} + 0.1) + (\rho_{SWIR} + 0.02)} = \frac{(Band2 + 0.1) - (Band6 + 0.02)}{(Band2 + 0.1) + (Band6 + 0.02)}$	[28]

2.5. The Ratio between NDVI and Surface Temperature

Several studies demonstrated that the combined use of NDVI and surface temperature (ST) provides stronger relationships with water content than either of the two variables alone [5,23,67,68]. A positive correlation between the NDVI/ST ratio and fuel moisture is expected [67] and we use in this study the NDVI/ST ratio to predict vegetation water content.

The Normalized Difference Vegetation Index was computed from MODIS reflectance data using NIR and red bands as following [69]:

$$NDVI = \frac{\rho_{NIR} - \rho_{RED}}{\rho_{NIR} + \rho_{RED}} = \frac{Band2 - Band1}{Band2 + band1}$$

The 500-m NDVI data were re-sampled to 1 km using the Nearest Neighbor algorithm to facilitate comparison with MODIS LST 1-km data.

The MYD11 L3 land surface temperature (LST) product, produced by NASA using the Generalized Split-Window (GSW) algorithm [70], is based on brightness temperatures measured in bands #31 (10.780–11.280 μm) and #32 (11.770–12.270 μm).

2.6. Statistical Analyses

All statistical analyses were carried out using the software R [53], and $P < 0.05$ was used to determine the significance of all tests. A correlation matrix was used to determine the satellite indices that were most highly correlated with the herbaceous water content measured in the field. Linear relationships were calculated between VIs and the ratio of NDVI/ST that correlated best with field measurements. Correlograms were performed to check for autocorrelation between observations and residuals from linear regression models were checked for normality and homoscedasticity [71].

Finally, the potential application of detecting changes in herbaceous water content at the end of the rainy season during the early fire-season was tested. For this, the best relationship computed using *in situ* measurements and the VIs from the eight-day MODIS surface reflectance data (covering the period of 6 October to 23 November 2010) was used to estimate the herbaceous water content changes over the country.

3. Results

3.1. Spatial and Temporal Evolution of Herbaceous Water Content from Field Measurements

During the 32 days of sampling collection of biomass for herbaceous water content estimates, the EWT results showed that the herbaceous water content increased from the north (Sahelian savannas) to the south (Sudanian savannas) following the rainfall gradient (Figure 4). The average values of EWT ranged between 0.011 and 0.045 g·cm^{-2} for the three sites over the 6 October to 23 November 2010 period, with the highest EWT values (mean and variability) recorded at the southernmost location (Figure 4(top)). The temporal evolution of the water content was characterized by a continued downward trend for all sites. 40 days after the last rain, the herbaceous vegetation in the northern site had almost lost all its water content (0.003 g·cm^{-2} being close to the dry weight), whereas it was

0.014 and 0.018 g·cm^{-2} at sites 2 and 3, respectively. Unlike EWT, the FMC results showed that the highest values of herbaceous water content were recorded at the central site, also characterized by the highest variability between sub-sites (Figure 4(bottom)).

Figure 4. Temporal evolution of herbaceous moisture content from field observations at the three sites (Figure 1) using two metrics: Equivalent water thickness (EWT) (**top**) and fuel moisture content (FMC) (**bottom**). Measurements covered the period from 6 October to 23 November 2010. Day 1 corresponded to eight days after the last rain. Error bars (based on one standard deviation) represent the daily variability of moisture content from the nine plots in the experimental design.

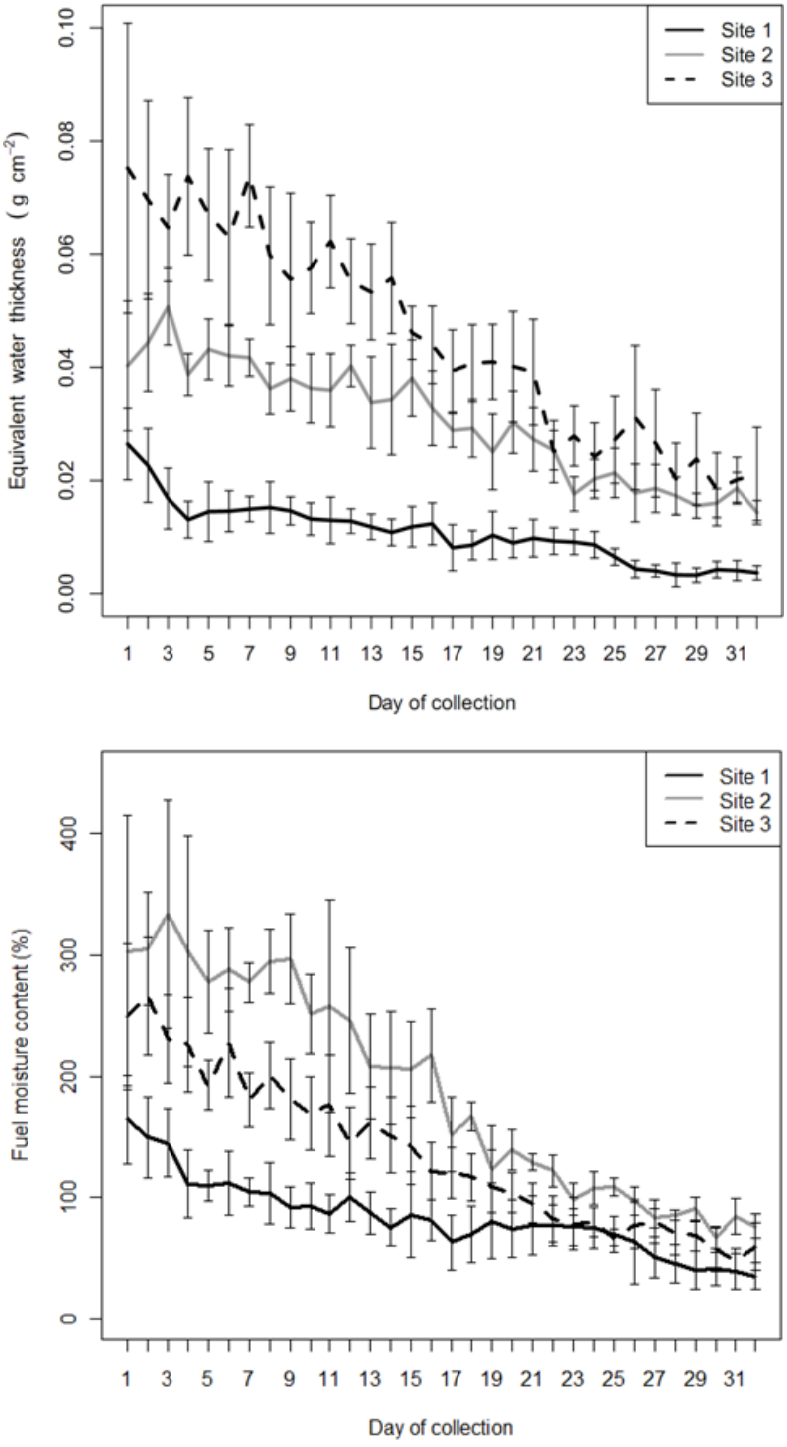

3.2. Relationship between VIs and Field Measurements of Herbaceous Water Content

At the site level, the vegetation indices $NDII_{(2.6)}$, $MSI_{(6.2)}$, $GVMI_{(2.6)}$ and NDVI/ST (computed from daily data) were in most cases highly correlated with both EWT and FMC (Table 3). The results showed that FMC is important for herbaceous water content assessment at the individual site level while EWT was found efficient at the site level and across site comparisons. Correlations between field measurements of water content and VIs decreased along the latitudinal gradient from the northernmost Sahelian site (r varied from 0.84 to 0.96) towards the southward Sudanian sites (r = 0.27–0.90 and 0.02–0.95 for sites 2 and 3, respectively) (Table 3).

Table 3. Correlation coefficients between field measurements of herbaceous moisture content and (1) vegetation indices and (2) ratio NDVI/ST. Fuel Moisture Content (FMC), Equivalent Water Thickness (EWT), Moisture Stress Index (MSI), Normalized Difference Infrared Index (NDII), Normalized Difference Water Index (NDWI), Global Vegetation Moisture Index (GVMI), Simple Ratio Water Index (SRWI), Normalized Difference Vegetation Index (NDVI), Surface Temperature (ST).

Vegetation Satellite Indices		Vegetation Indices							
		Site 1		Site 2		Site 3		All Sites	
		FMC	EWT	FMC	EWT	FMC	EWT	FMC	EWT
$MSI_{(6,2)}$	r	−0.92	−0.91	−0.82	−0.89	−0.80	−0.81	−0.62	−0.88
$MSI_{(7,2)}$	r	−0.92	−0.90	−0.44	−0.47	−0.60	−0.61	−0.46	−0.79
$NDII_{(2,6)}$	r	0.93	0.92	0.84	0.90	0.76	0.78	0.63	0.90
$NDII_{(2,7)}$	r	0.91	0.88	0.39	0.42	0.59	0.60	0.42	0.79
$NDWI_{(2,5)}$	r	0.85	0.84	−0.27	−0.30	0.94	0.95	0.08	0.11
$GVMI_{(2,6)}$	r	0.93	0.92	0.84	0.90	0.80	0.81	0.62	0.90
$SRWI_{(2,5)}$	r	0.85	0.84	−0.35	−0.39	−0.03	0.02	−0.08	−0.04
NDVI/ST	r	0.96	0.95	0.62	0.65	0.74	0.69	0.52	0.85

Based on the best correlations of EWT (as compared to FMC) with field observations, it was chosen only to focus on EWT estimates in the linear regression models for predicting vegetation water content from remote sensing data. The linear relationships between EWT and VIs derived from daily MODIS Aqua data were all highly significant ($p < 0.001$) with r^2 varying from 0.78 with $MSI_{(6,2)}$ to 0.81 and 0.82 with $GVMI_{(2,6)}$ and $NDII_{(2,6)}$, respectively (Figure 5), while the linear relationship between EWT *vs.* NDVI/ST was weaker ($r^2 = 0.72$, $p < 0.001$). When testing for normality, homoscedasticity and temporal autocorrelation all assumptions were met. The use of daily MODIS data might potentially be influenced by day-to-day variations in sun-target-sensor geometry having a wavelength specific impact on reflectance's (and VIs) due to wavelength-dependent differences in the anisotropy factor [35,72]. We also used the eight-day MODIS composite data related to field data synthesized into eight-day data (by temporal averaging). The linear regression based on eight-day MODIS composite data and eight-day average values of field measured EWT showed significantly stronger relationships (Figure 5) with index values of $MSI_{(6,2)}$, $NDII_{(2,6)}$ and $GVMI_{(2,6)}$ explaining 81, 88, and 88% of the EWT variability, respectively.

Figure 5. Linear relationship between field observations of equivalent water thickness (EWT), vegetation indices and land surface temperature. Black dots and line represent the daily data while gray dots and dashed line represent the eight-day composite data.

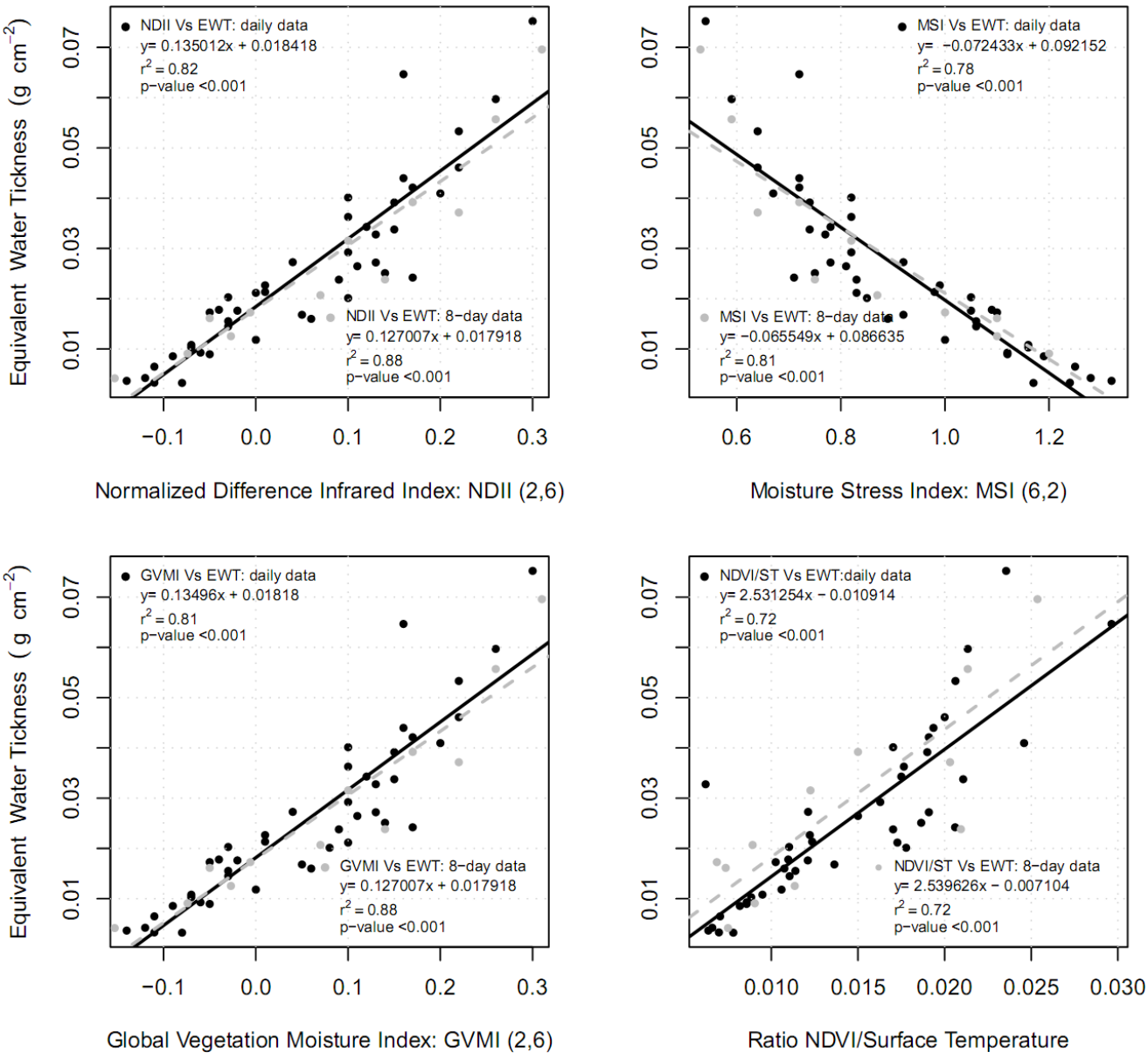

3.3. Application

Maps of estimated herbaceous fuel water content over Senegal were calculated using the strong significant relation found between eight-day $NDII_{(2,6)}$ and EWT. The six consecutive eight-day periods confirmed that the drying of vegetation followed a regional north–south gradient (Figure 6).

The monotonous trend in herbaceous water content reduction in the Senegalese savanna landscapes evolved from largely lush herbaceous vegetation (Doy 273–280) to widely senescent herbaceous vegetation with very limited water content (Doy 313–320), with a temporal lag related to geographical location (from North to South).

Figure 6. Changes in vegetation moisture content from DOY (day of year) 273 to 320. EWT was retrieved from eight-day MODIS using the equation of the linear regression between NDII and field measured EWT (Figure 5 top left).

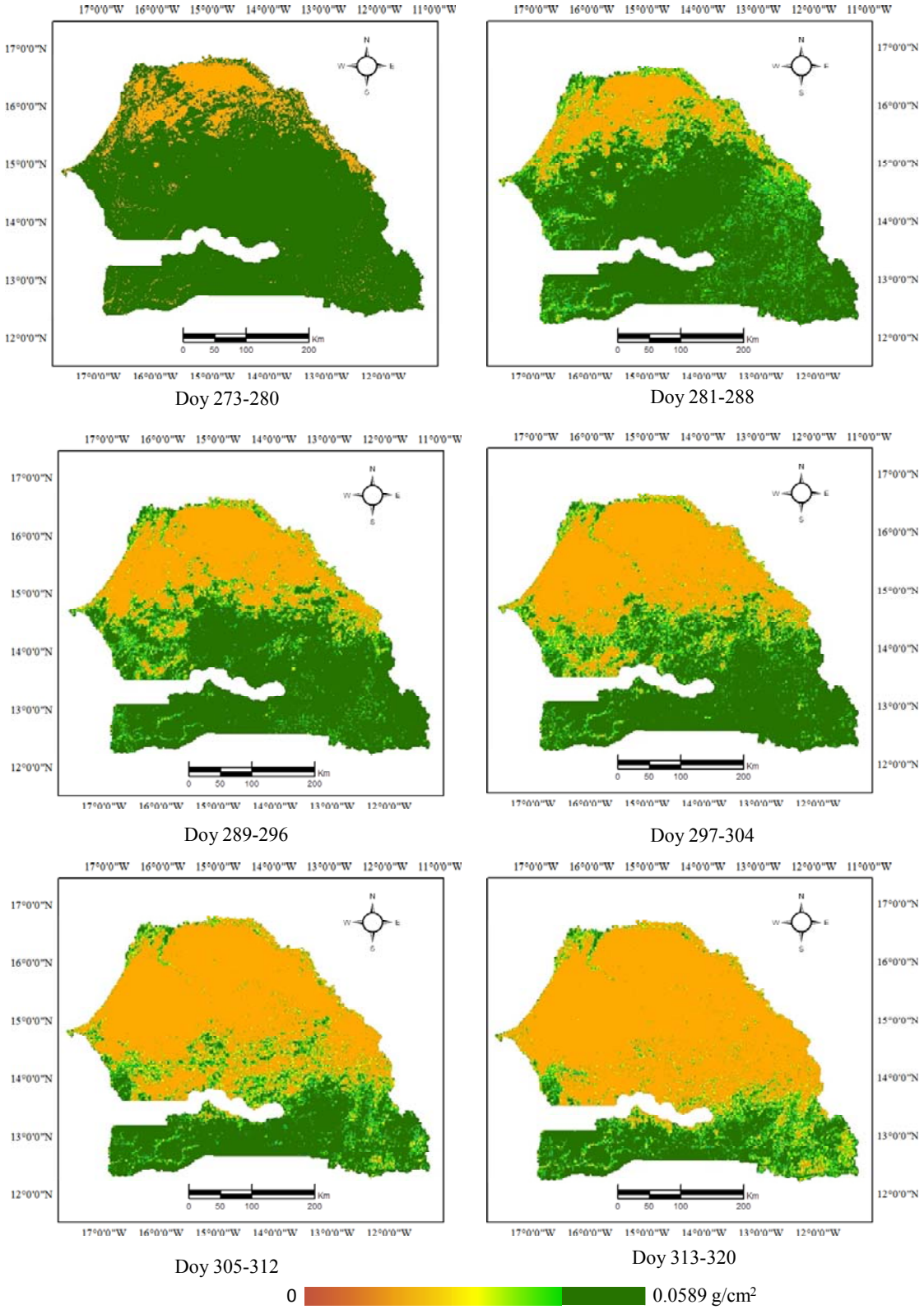

4. Discussion

4.1. Remote Sensing Indices versus Field Reality and Complexity

According to Dauriac [29], the estimation of vegetation water content is an approximation regardless of methods used (field measurements or remote sensing). Especially in the case of dominant herbaceous vegetation (Sahelian site) being more sensitive to soil moisture, topography and weather conditions than woody vegetation (also present in Sudanian sites) this assertion could be valid. In addition, the presence of a mixture of several species of annual and perennial grasses, with different abilities regarding the mechanisms for regulation of water loss, is often characterized by different levels of water content at a given time. This is why it was mandatory to obtain representative samples as outlined in Section 2.2 to take into account the local variations.

EWT is difficult to operationally measure in the field, because it requires the calculation of leaf area [51]. Herbaceous leaf area (A) was measured visually in the field. Although visual estimation of some parameters on the herbaceous vegetation is common [73–75], the visual estimation of A could affect the accuracy of the results presented.

Despite these potential uncertainties, our results showed a consistent relationship over the studied region between VIs based on NIR/SWIR and EWT as many studies have found previously for different ecosystems [25,30,31,36,50,52]. Furthermore, strong correlations between FMC and VIs (NDII, GVMI and MSI) were found for each site, showing the possibility provided by remote sensing to predict FMC in areas where floristic composition is relatively uniform. However, we confirm that for Sahelian and Sudanian savannas, the relationship between FMC and VIs is relatively weaker at the overall level (analyzing all sites together) than at the local level (by site). Several earlier studies showed that estimation of FMC from reflectance measurements was challenging because FMC does not only depend on water absorption, but also on the changes in the dry matter as leafs dries [42]. The relationships between VI and FMC are likely to be species-specific and knowledge of the mixture of species and their biophysical properties (leaf internal structure) would be useful in estimating spatial variation in FMC from NIR/SWIR-based indices [52]. In fact, FMC expresses the intrinsic water content of plant which is partly related to the specific capacity of each plant species to regulate water loss. In addition, the use of 500-m and 1-km data for analysis of savanna ecosystems where vegetation type often varies at the scale of hectares rather than square kilometers could introduce uncertainties in the comparison between remotely sensed information and field observations.

Although the relationships between the ratio NDVI/ST and EWT were relatively strong ($r^2 = 0.72$), the following VIs ($NDII_{(2,6)}$, $GVMI_{(2,6)}$, $MSI_{(6,2)}$) tested generally provided the most satisfactory results on predicting herbaceous water content. All the indices, using the bands 2 and 6 located respectively in the NIR (where water absorption is weak) and SWIR (where water absorption is strong) wavelengths were found to be highly correlated with the field measurements of EWT and therefore deemed useful in estimating herbaceous water content. As part of the validation of GVMI in Senegal, Ceccato *et al.* [27] found that this index was suitable to predict vegetation water content with coefficients of correlation which ranged between 0.76 to 0.98. They [27] recommended, however, that the GVMI should be validated further with more field measurements in a range of different savanna ecosystems. Our study focused in part on this perspective and the results confirm those found by Ceccato *et al.* [27]. In

addition, the study of Ceccato *et al.* [27] was based on 10-day SPOT-VEGETATION (VGT) composite data covering the entire year whereas our study was targeting the period of the early dry season where most fires are recorded in Senegal, hence requiring daily monitoring of vegetation status for timely savanna fire management. We opted for MODIS data because of the improved temporal (if combining MODIS Terra and Aqua acquisitions), spectral and spatial resolution as compared to VGT data. MODIS freely provides two images per day (MODIS Terra and Aqua) with spatial resolution of 250–500 m in contrast to VGT imagery being provided as 10-day composite data free of charge at 1 km^2 resolution with a three-month dissemination delay.

The correlations between EWT/FMC and VI decreased moderately with decreasing aridity from north (site 1) to south (site 3). This difference was most likely related to the site-specific differences in tree cover: with a low woody cover (11%) at site 1, 29% at site 2 and more closed woody cover (50%) at site 3. This suggests that such NIR/SWIR-based indices are less successful in the estimating of herbaceous water content for more dense woody cover. During the period of herbaceous senescence (as studied here) woody foliage will typically retain water from deep root water access. Optical satellite remote sensing methods have limited capabilities of separating the reflectance signal of herbaceous and forest canopy, when both layers are still green and when the sub-canopy herbaceous layer withers below a green forest canopy. Hence, the reduced ability of NIR/SWIR VIs to explain the variability in EWT is to be expected for an increased woody cover.

4.2. Applied Remote Sensing Tools on Savanna Surveillance

Overall, the drying of herbaceous vegetation followed a regional north–south gradient mirroring the withdrawal of rains (controlled by the movement of the Intertropical Convergence Zone (ITCZ)) from north to south. Figure 6 shows a rapid decrease of herbaceous water content over a period of six weeks. These results corroborated the findings of Verbesselt *et al.* [11] who indicated that the transition from wet to dry savanna vegetation occurs fast (approximately 1–2 months).

Forest fire managers have traditionally collected *in situ* data on FMC because it is relatively easy to measure in the field and because FMC is closely related to ignition probability influencing the rate of spread if a fire occurs [52]. Our results suggest the effectiveness of using EWT when assessing herbaceous water content by satellite remote sensing. The mapping of EO-based herbaceous water content conducted in this study highlighted the potential usefulness for forest managers. However, the NIR/SWIR-based index method suggested here should be tested for a larger number of sites to further study the influence of species dependency on using either EWT or FMC as a metric for herbaceous water content.

5. Conclusion

In this study, satellite remote sensing has proven useful for estimating herbaceous water content. Vegetation indices computed using MODIS bands 2 (0.858 μm) and 6 (1.640 μm) located in the near-infrared (NIR) and shortwave infrared (SWIR) wavelengths, respectively, showed a strong significant relationship with leaf equivalent water thickness (EWT) for different sites representative of different Sahelian and Sudanian savanna ecosystems. This relationship was found to decrease moderately as a function of the woody cover as reflected by the selection of the three sites ranging

from sparse woody cover (<11%) in the north, to medium dense woody cover (approximately 50%) in the southernmost site. Remote sensing has proven to be a powerful tool for monitoring the drying process of herbaceous vegetation. Looking at the results, remote sensing could provide a good opportunity for forest managers in the assessment of herbaceous water content. In addition, this information is useful because of the importance of herbaceous water content in the management of savanna fires.

Acknowledgements

This work received financial support from the French International Cooperation (French Embassy in Senegal), the International Foundation for Science (IFS), the Senegal Government through the "Fonds d'Impulsion pour la Recherche Scientifique et Technique" (FIRST program), the U3E Project of the University Cheikh Anta Diop of Dakar and French International Cooperation, and the West African Network for Studies of Environmental Change (Wansec)/DANIDA.

We thank NASA for the providing of MODIS data, the laboratory of Senegalese Ministry of Mines where the biomass samples were dried. We thank also Fabien Tinquaut for his help in automating the processing of satellite images, and the four anonymous reviewers for their very helpful comments and suggestions.

Conflict of Interest

The authors declare no conflict of interest.

References

1. Heinl, M.; Frost, P.; Vanderpost, C.; Sliva, J. Fire activity on drylands and floodplains in the southern Okavango Delta, Botswana. *J. Arid Environ.* **2007**, *68*, 77–87.
2. Jacquin, A.; Sheeren, D.; Lacombe, J.-P. Vegetation cover degradation assessment in Madagascar savanna based on trend analysis of MODIS NDVI time series. *Int. J. Appl. Earth Obs. Geoinf.* **2010**, *12*, 3–10.
3. Goldammer, J.G.; Crutzen, P.J. Fire in the Environment: Scientific Rationale and Summary of Results of the Dahlem Workshop. In *Fire in the Environment: The Ecological Atmospheric and Climatic Importance of Vegetation Fires*; Crutzen, J.P., Ed.; John Wiley & Sons: Chichester, UK, 1993; pp. 1–14.
4. Maki, M.; Ishiahra, M.; Tamura, M. Estimation of leaf water status to monitor the risk of forest fires by using remotely sensed data. *Remote Sens. Environ.* **2004**, *90*, 441–450.
5. Chuvieco, E.; Cocero, D.; Riaño, D.; Martin, P.; MartíNez-Vega, J.; de La Riva, J.; Pérez, F. Combining NDVI and surface temperature for the estimation of live fuel moisture content in forest fire danger rating. *Remote Sens. Environ.* **2004**, *92*, 322–331.
6. Nelson, R.M. Water Relations in Forest Fuels. In *Forest Fires: Behavior and Ecological Effects*; Johnson, E.A., Miyanishi, K., Eds.; Academic Press: San Francisco, CA, USA, 2001; pp. 79–143.
7. Viegas, D.X.; Viegas, T.P.; Ferreira, A.D. Moisture content of fine forest fuels and fire occurrence in Central Portugal. *Int. J. Wildland Fire* **1992**, *2*, 69–85.

8. Dasgupta, S.; Qu, J.J.; Hao, X.; Bhoi, S. Evaluating remotely sensed live fuel moisture estimations for fire behavior predictions in Georgia, USA. *Remote Sens. Environ.* **2007**, *108*, 138–150.
9. Savadogo, P.; Zida, D.; Sawadogo, L.; Tiveau, D.; Tigabu, M.; Odén, P.C. Fuel and fire characteristics in savanna-woodland of West Africa in relation to grazing and dominant grass type. *Int. J. Wildland Fire* **2007**, *16*, 531–539.
10. Mulqueeny, C.M.; Goodman, P.S.; O'connor, T.G. Determinants of inter-annual variation in the area burnt in a semiarid African savanna. *Int. J. Wildland Fire* **2011**, *20*, 532–539.
11. Verbesselt, J.; Somers, B.; Lhermitte, S.; Jonckheere, I.; van Aardt, J.; Coppin, P. Monitoring herbaceous fuel moisture content with SPOT VEGETATION time-series for fire risk prediction in savanna ecosystems. *Remote Sens. Environ.* **2007**, *108*, 357–368.
12. Chen, D.; Huang, J.; Jackson, T.J. Vegetation water content estimation for corn and soybeans using spectral indices derived from MODIS near- and short-wave infrared bands. *Remote Sens. Environ.* **2005**, *98*, 225–236.
13. Davidson, A.; Wang, S.; Wilmshurst, J. Remote sensing of grassland-shrubland vegetation water content in the shortwave domain. *Int. J. Appl. Earth Obs. Geoinf.* **2006**, *8*, 225–236.
14. Yilmaz, M.T.; Hunt, E.R., Jr.; Jackson, T.J. Remote sensing of vegetation water content from equivalent water thickness using satellite imagery. *Remote Sens. Environ.* **2008**, *112*, 2514–2522.
15. Yilmaz, M.T.; Hunt, E.R., Jr.; Goins, L.D.; Ustin, S.L.; Vanderbilt, V.C.; Jackson, T.J. Vegetation water content during SMEX04 from ground data and Landsat 5 Thematic Mapper imagery. *Remote Sens. Environ.* **2008**, *112*, 350–362.
16. Fensholt, R.; Sandholt, I. Derivation of a shortwave infrared water stress index from MODIS near- and shortwave infrared data in a semiarid environment. *Remote Sens. Environ.* **2003**, *87*, 111–121.
17. Chuvieco, E.; Riano, D.; Aguado, I.; Cocero, D. Estimation of fuel moisture content from multitemporal analysis of Landsat Thematic Mapper reflectance data: Applications in fire danger assessment. *Int. J. Remote Sens.* **2002**, *23*, 2145–2162.
18. Verbesselt, J.; Somers, B.; van Aardt, J.; Jonckheere, I.; Coppin, P. Monitoring herbaceous biomass and water content with SPOT VEGETATION time-series to improve fire risk assessment in savanna ecosystems. *Remote Sens. Environ.* **2006**, *101*, 399–414.
19. Tucker, C.J. Asymptotic nature of grass canopy spectral reflectance. *Appl. Opt.* **1977**, *16*, 1151–1156.
20. Illera, P.; Fernandez, A.; Delgado, J.A. Temporal evolution of the NDVI as an indicator of forest fire danger. *Int. J. Remote Sens.* **1996**, *17*, 1093–1105.
21. Burgan, R.E. Use of remotely sensed data for fire danger estimation. *EARSeL Adv. Remote Sens.* **1996**, *4*, 1–8.
22. Burgan, R.E.; Hartford, R.A. Live Vegetation Moisture Calculated from NDVI and Used in fire Danger Rating. In Proceedings of the 13th Conference on Fire and Forest Meteorology, Lorne, Australia, 27–31 October 1997; pp. 225–231.

23. Chuvieco, E.; Deshayes, M.; Stach, N.; Cocero, D.; Riano, D. Short-Term Fire Risk: Foliage Moisture Content Estimation from Satellite Data. In *Remote Sensing of Large Wildfires in the European Mediterrranean Basin*; Chuvieco, E., Ed.; Springer-Verlag: Berlin, Germany, 1999; pp. 17–38.
24. Paltridge, G.W.; Barber, J. Monitoring grassland dryness and fire potential in Australia with NOAA/AVHRR data. *Remote Sens. Environ.* **1988**, *25*, 381–394.
25. Ceccato, P.; Flasse, S.; Tarantola, S.; Jacquemoud, S.; Grégoire, J.-M. Detecting vegetation leaf water content using reflectance in the optical domain. *Remote Sens. Environ.* **2001**, *77*, 22–33.
26. Larcher, W. *Physiological Plant Ecology. Ecophysiology and Stress Physiology of Functional Groups*, 3rd ed.; Springer: New York, NY, USA, 1995; p. 528.
27. Ceccato, P.; Flasse, S.; Grégoire, J.-M. Designing a spectral index to estimate vegetation water content from remote sensing data Part 2. Validation and applications. *Remote Sens. Environ.* **2002**, *82*, 198–207.
28. Ceccato, P.; Gobron, N.; Flasse, S.; Pinty, B.; Tarantola, S. Designing a spectral index to estimate vegetation water content from remote sensing data: Part 1 Theoretical approach. *Remote Sens. Environ.* **2002**, *82*, 188–197.
29. Dauriac, F. Suivi Multi-Echelle par Télédétection et Spectroscopie de L'état Hydrique de la Végétation Méditerranéenne Pour la Prévention du Risque de Feu de Forêt. Ph.D. Thesis, ENGREF (Ecole Nationale du Génie Rural, des Eaux et Forêts), Centre de Montpellier, Montpellier, France, 2004.
30. Cheng, Y.-B.; Zarco-Tejada, P.J.; Riaño, D.; Rueda, C.A.; Ustin, S.L. Estimating vegetation water content with hyperspectral data for different canopy scenarios: Relationships between AVIRIS and MODIS indexes. *Remote Sens. Environ.* **2006**, *105*, 354–366.
31. Zarco-Tejada, P.J.; Rueda, C.A.; Ustin, S.L. Water content estimation in vegetation with MODIS reflectance data and model inversion methods. *Remote Sens. Environ.* **2003**, *85*, 109–124.
32. Cheng, Y.-B.; Wharton, S.; Ustin, S.L.; Zarco-Tejada, P.J.; Falk, M.; Kyaw, K.T.P.U. Relationships between Moderate Resolution Imaging Spectroradiometer water indexes and tower flux data in an old-growth conifer forest. *J. Appl. Remote Sens.* **2007**, *1*, 1–26.
33. Cheng, Y.-B.; Ustin, S.L.; Riaño, D.; Vanderbil, V.C. Water content estimation from hyperspectral images and MODIS indexes in Southeastern Arizona. *Remote Sens. Environ.* **2008**, *112*, 363–374.
34. Houborg, R.; Soegaard, H.; Boegh, E. Combining vegetation index and model inversion methods for the extraction of key vegetation biophysical parameters using Terra and Aqua MODIS reflectance data. *Remote Sens. Environ.* **2007**, *106*, 39–58.
35. Fensholt, R.; Huber, S.; Proud, S.R.; Mbow, C. Detecting canopy water status using shortwave infrared reflectance data from polar orbiting and geostationary platforms. *IEEE J. Sel. Top. Appl. Earth Obs. Remote Sens.* **2010**, *3*, 271–285.
36. Serrano, L.; Ustin, S.L.; Roberts, D.A.; Gamon, J.A.; Peñuelas, J. Deriving water content of chaparral vegetation from AVIRIS data. *Remote Sens. Environ.* **2000**, *74*, 570–581.
37. Goetz, S.J. Multisensor analysis of NDVI, surface temperature and biophysical variables at a mixed grassland site. *Int. J. Remote Sens.* **1997**, *18*, 71–94.

38. Jackson, R.D.; Reginato, R.J.; Idso, S.B. Wheat canopy temperature: A practical tool for evaluating water requirements. *Water Resour. Res.* **1977**, *13*, 651–656.
39. Tucker, C.J. Red and photographic infrared linear combinations for monitoring vegetation. *Remote Sens. Environ.* **1979**, *8*, 127–150.
40. Goward, S.N.; Hope, A.S. Evapotranspiration from combined reflected solar and emitted terrestrial radiation: Preliminary FIFE results from AVHRR data. *Adv. Space Res.* **1989**, *9*, 239–249.
41. Nemani, R.R.; Pierce, L.L.; Running, S.W.; Goward, S.N. Developing satellite derived estimates of surface moisture status. *J. Appl. Meteorol.* **1993**, *28*, 276–284.
42. Chuvieco, E.; Wagtendonk, J.; Riaño, D.; Yebra, M.; Ustin, S.L. Estimation of Fuel Conditions for Fire Danger Assessment. In *Earth Observation of Wildland Fires in Mediterranean Ecosystems*; Springer-Verlag: Berlin/Heidelberg, Germany, 2009; pp. 83–96.
43. Sagna, P. Dynamisme du Climat et de Son Evolution Dans la Partie Ouest de L'Afrique Occidentale, Tome II. Thèse de doctorat d'Etat, Université Cheikh Anta Diop, Dakar, Sénégal, 2005.
44. Sow, M.; Hély, C.; Mbow, C.; Sambou, B. Fuel and fire behavior analysis for early-season prescribed fire planning in sudanian and sahelian savannas. *J. Arid Environ.* **2013**, *89*, 84–93.
45. Mahamane, A.; Saadou, M. Méthodes D'étude et D'analyse de la Flore et de la Végétation Tropicale. In *Actes de L'atelier sur L'Harmonisation des Méthodes*; Sustainable Use of Natural Vegetation in West Africa (SUN): Niamey, Niger, 2008; p. 70.
46. Akpo, L.E.; Banoin, M.; Grouzis, M. Effet de l'arbre sur la production et la qualité fourragères de la végétation herbacée: Bilan pastoral en milieu sahélien. *Revue Méd. Vét.* **2003**, *154*, 619–628.
47. Chuvieco, E.; Aguado, I.; Cocero, D.; Riaño, D. Design of an empirical index to estimate fuel moisture content from NOAA-AVHRR images in forest fire danger studies. *Int. J. Remote Sens.* **2003**, *24*, 1621–1637.
48. Chuvieco, E.; Aguado, I.; Dimitrakopoulos, A.P. Conversion of fuel moisture content values to ignition potential for integrated fire danger assessment. *Can. J. For. Res.* **2004**, *34*, 2284–2293.
49. Roberts, D.A.; Green, R.O.; Adams, J.B. Temporal and spatial patterns in vegetation and atmospheric properties from AVIRIS. *Remote Sens. Environ.* **1997**, *62*, 223−240.
50. Ustin, S.L.; Roberts, D.A.; Jacquemoud, S.; Gardner, M.; Scheer, G. Estimating canopy water content of chaparral shrubs using optical methods. *Remote Sens. Environ.* **1998**, *65*, 280−291.
51. Chuvieco, E.; Cocero, D.; Aguado, I.; Palacios, A.; Prado, E. Improving burning efficiency estimates through satellite assessment of fuel moisture content. *J. Geophys. Res.* **2004**, *109*, 1–8.
52. Danson, F.M.; Bowyer, P. Estimating live fuel moisture content from remotely sensed reflectance. *Remote Sens. Environ.* **2004**, *92*, 309–321.
53. R Development Core Team. *R: A Language and Environment for Statistical Computing*. Available online: http://www.R-project.org (accessed on 7 November 2011*)*.
54. Wu, C.; Niu, Z.; Tang, Q.; Huang, W. Estimating chlorophyll content from hyperspectral vegetation indices: Modeling and validation. *Agric. For. Meteorol.* **2008**, *148*, 1230–1241.
55. Wardlow, B.D.; Egbert, S.L.; Kastens, J.H. Analysis of time-series MODIS 250 m vegetation index data for crop classification in the U.S. Central Great Plains. *Remote Sens. Environ.* **2007**, *108*, 290–310.

56. Bannari, A.; Asalhi, H. *Sensitivity Analysis of Spectral Indices to Ozone Absorption Using Physical Simulations in a Forest Environment: Comparative Study between MODIS, SPOT VÉGÉTATION & AVHRR*. Avaiable online: http://www.isprs.org/proceedings/XXXV/congress/comm7/papers/157.pdf (accessed on 6 May 2013).
57. Lyon, J.G.; Yuan, D.; Lunetta, R.S.; Elvidg, C.D. A change detection experiment using vegetation indices. *Photogramm. Eng. Remote Sensing* **1998**, *64*, 143–150.
58. Gitelson, A.A.; Kaufman, Y.J.; Stark, R.; Rundquist, D. Novel algorithms for remote estimation of vegetation fraction. *Remote Sens. Environ.* **2002**, *80*, 76–87.
59. Gao, B.-C. NDWI—A normalized difference water index for remote sensing of vegetation liquid water from space. *Remote Sens. Environ.* **1996**, *58*, 322–331.
60. Hardisky, M.A.; Klemas, V.; Smart, R.M. The influences of soil salinity, growth form, and leaf moisture on the spectral reflectance of Spartina alterniflora canopies. *Photogramm. Eng. Remote Sensing* **1983**, *49*, 77–83.
61. Hunt, R.E.; Rock, R.N. Detection of changes in leaf water content using near-and middle-infrared reflectances. *Remote Sens. Environ.* **1989**, *30*, 43–54.
62. Jackson, T.J.; Chen, D.; Cosh, M.; Li, F.; Anderson, M.; Walthall, C.; Doriaswamy, P.; Hunt, E.R. Vegetation water content mapping using Landsat data derived normalized difference water index for corn and soybeans. *Remote Sens. Environ.* **2004**, *92*, 475–482.
63. Zarco-Tejada, P.J.; Ustin, S.L. Modeling Canopy Water Content for Carbon Estimates from MODIS Data at Land EOS Validation Sites. In Proceedings of the IEEE 2001 International Geoscience and Remote Sensing Symposium, Sydney, Australia, 9–13 July 2001; pp. 342–344.
64. Guerschman, J.P.; van Dijk, A.I.J.M.; Albert, I.J.M.; Mattersdorf, G.; Beringer, J.; Hutley, L.B.; Leuning, R.; Pipunic, R.C.; Sherman, B.S. Scaling of potential evapotranspiration with MODIS data reproduces flux observations and catchment water balance observations across Australia. *J. Hydrol.* **2009**, *369*, 107–119.
65. Vermote, E.F.; El Saleous, N.Z.; Justice, C.O. Atmospheric correction of MODIS data in the visible to middle infrared: First results. *Remote Sens. Environ.* **2002**, *83*, 97–111.
66. Vermote, E.F.; Saleous, N.E.; Justice, C.O.; Kaufman, Y.J.; Privette, P.J.; Remer, L.; Roger, J.C.; Tanré, D. Atmospheric correction of visible to middle-infrared EOS-MODIS data over land surfaces: Background, operational algorithm and validation. *J. Geophys. Res.* **1997**, *102*, 17131–17141.
67. Alonso, M.; Camarasa, A.; Chuvieco, E.; Cocero, D.; Iksu, A.K.; Martin, M.P.; Salas, F.J. Estimating temporal dynamics of fuel moisture content of Mediterranean species from NOAA-AVHRR data. *EARSel Adv. Remote Sens.* **1996**, *4*, 9–24.
68. Prosper-Laget, V.; Douguédroit, A.; Guinot, J.P. Mapping the risk of forest fire occurrence using NOAA satellite information. *EARSeL Adv. Remote Sens.* **1995**, *4*, 30–38.
69. Rouse, J.W.; Hass, R.H.; Schell, J.A.; Deering, D.W. Monitoring Vegetation Systems in the Great Plains with ERTS. In Proceedings of the 3rd Earth Resources Technology Satellite-1 Symposium, Greenbelt, MD, USA, 10–14 December 1973; NASA SP-351, pp. 309–317.
70. Wan, Z.; Dozier, J. A generalized split-window algorithm for retrieving land surface temperature from space. *IEEE Trans. Geosci. Remote Sens.* **1996**, *34*, 892–905.

71. Scherrer, B. *Biostatistique*, 2nd ed.; Les éditions de la Chenelière Inc.: Montréal, QC, Canada, 2007; Volume 1, p. 816.
72. Fensholt, R.; Sandholt, I.; Proud, S.R.; Stisen, S.; Rasmussen, M.O. Assessment of MODIS sun-sensor geometry variations effect on observed NDVI using MSG SEVIRI geostationary data. *Int. J. Remote Sens.* **2010**, *31*, 6163–6187.
73. Anderson, S.A.J.; Anderson, W.R.; Hollis, J.J.; Botha, E.J. A simple method for field-based grassland curing assessment. *Int. J. Wildland Fire* **2011**, *20*, 804–814.
74. Millie, S.; Adams, R. Measures of Grassland Curing: A Comparison of Destructive Sampling with Visual and Satellite Estimates. In Proceedings of the Australian Bushfire 99 Conference, Albury, Auatralia, 7–9 July 1999; pp. 257–263.
75. Catchpole, W.R.; Wheeler, C.J. Estimating plant biomass: A review of techniques. *Austr. J. Ecol.* **1992**, *17*, 121–131.